Spatially Distributed Multi-Period Optimal Power Flow with Battery Energy Storage Systems

Aryan Ritwajeet Jha∗, *SIEEE*, Subho Paul†, *MIEEE*, and Anamika Dubey∗, *SMIEEE*
∗*School of Electrical Engineering & Computer Science*, *Washington State University*, Pullman, WA, USA
†*Department of Electrical Engineering*, *Indian Institute of Technology (BHU) Varanasi*, Varanasi, UP, India
∗{aryan.jha, anamika.dubey}@wsu.edu, †{subho.eee}@iitbhu.ac.in

***Abstract*—The growing presence of battery-based distributed energy resources (DERs) in power distribution systems necessitates the development of multi-period optimal power flow (MPOPF) algorithms. Generally, an MPOPF problem is formulated as a mixed integer non-convex programming (MINCP) problem and solved in centralized manner. The centralized solutions for MPOPF problem, termed as MPCOPF, suffer from scalability challenges. A typical solution time for a medium-sized (∼100 bus system) is in the order of 10^3 to 10^4 seconds; such solution time-scales are too slow for operational decision-making. This paper introduces a spatially distributed algorithm to solve MPOPF problems, termed MPDOPF, designed to address these shortcomings. Our method breaks down the centralized MPOPF problem into smaller sub-problems, which are solved in parallel. We achieve network-level optimality using the Equivalent Network Approximation (ENApp) algorithm, where neighboring agents iteratively exchange boundary voltage and power flow variables until convergence. We analyze the performance of the proposed MPDOPF algorithm using the IEEE 123 bus test system, providing insights into the advantages of distributed MPOPF frameworks in terms of solution time compared to centralized approaches.**

***Index Terms*—Battery energy storage systems, distribution system, optimal power flow, distributed energy resources.**

I. Introduction

Optimal power flow (OPF) methods are employed to optimally coordinate grid's controllable resources for different system-level objectives, such as economic operations, reliability, and resilience. The significance of OPF studies is growing in relevance at the distribution system level, driven by the increasing adoption of distributed energy resources (DERs), particularly photovoltaic systems (PVs) and battery energy storage systems (BESS). Furthermore, the adoption of BESS is gaining significance for managing the variability of DERs through controlled charging and discharging, thereby ensuring supply-demand balance [1]. Incorporating BESS into OPF problems substantially raises the complexity of network optimization problems, transitioning from a single-period, time-decoupled OPF to a multi-period, time-coupled OPF.

Traditionally, centralized OPF (COPF) methods have been widely used, where a central controller processes aggregated grid-edge data, executes the OPF algorithm, and sends control signals to manage resources [2]. The COPF algorithms for DER management are generally developed as a mixed integer non-convex programming (MINCP) problem and then simplified either as a convex problem by adopting second-order cone programming (SOCP) relaxations [3] [4], or as a linear problem by adopting Taylor series expansion [2], polyhedral approximations [5] or linear power flow models [6]. Unfortunately, COPF methods pose scalability challenges for larger networks and for difficult classes of OPF problems such multi-period time-coupled formulations required to optimally manage BESS.

To address scalability challenges, distributed OPF (DOPF) algorithms have been introduced. These algorithms decompose the COPF problem into smaller sub-problems that are solved concurrently, leveraging communication among neighboring areas. In this context, the Auxiliary Problem Principle (APP) and the Alternating Direction Method of Multipliers (ADMM) are widely adopted algorithms for solving various OPF problems, including non-convex formulations [7], convex-relaxed versions [8]–[10], and linear approximations [11]. Similarly, in a prior study [12], the authors' research group introduced a DOPF framework utilizing the Equivalent Network Approximation method (ENApp). This approach was shown to require fewer macro iterations compared to traditional ADMM or APP algorithms for solving DOPF problems.

The above references [3]- [11] mainly focused on solving single time-period OPF problems and did not include the coordination of grid-edge devices that introduce time-coupled constraints, such as BESS. The inclusion of BESS models results in a multi-period OPF (MPOPF) problem with time-coupled constraints. Reference [13] proposed a nonlinear multi-period centralized OPF (MPCOPF) approach to optimally coordinate active-reactive power dispatch from batteries and DERs in distribution systems. Alizadeh and Capitanescu [14] proposed a stochastic security-constrained MPCOPF, which sequentially solves a specific number of linear approximations of the original problem. Usman and Capitanescu [15] developed three different MPCOPF frameworks. All three approaches begin by solving a linear program to optimize the binary variables first, followed by either a linear or non-linear program to optimize the continuous variables. Optimal battery schedules are determined in [16] considering uncertain renewable power generation by solving an MPCOPF. A bi-level robust MPCOPF is suggested in [17] for determining active and reactive power dispatches from the grid edge devices. Wu et al. [18] framed a Benders Decomposition (BD) based multi-period distributed OPF (MPDOPF) after decomposing the original centralized multi-parametric quadratic problem into one master and multiple sub-problems.

TABLE I: TAXONOMY TABLE FOR COMPARISON

References	DERs	Batteries	Single period OPF	Multi-period OPF	Centralized OPF	Distributed OPF	Framework
[3], [4]			✓		✓		Convex
[5]	✓		✓		✓		Linear
[6]			✓		✓		Linear
[7]	✓		✓			✓	Convex (APP)
[8]- [10]	✓		✓			✓	Convex (ADMM)
[11]	✓		✓			✓	Linear (ADMM)
[12]	✓		✓			✓	Non-convex (ENApp)
[13]	✓	✓		✓	✓		Non-convex
[14]–[17]	✓	✓		✓	✓		Linear/convex
[18]	✓	✓		✓		✓	Quadratic (BD)
This paper	✓	✓		✓		✓	Non-convex (ENApp)

Over recent years, numerous research efforts have focused on developing MPOPF methodologies. However, the following research gaps persist.

1) The MPOPF models are mainly solved centrally [13]-[17]. The centralized methods suffer from scalability and computational challenges, requiring significantly long solution times, rendering them unsuitable for operational decision-making.
2) Reference [18] proposed a MPDOPF framework using Benders Decomposition. However, this approach suffers from slow convergence and needs a central controller to solve the master problem.

This article aims to address the above research gaps by developing a spatially distributed MPOPF (MPDOPF) framework. The distribution system is divided into multiple connected areas, each solving its own local MPOPF problem and periodically communicating the values of boundary variables with neighboring areas. The interaction between the areas is modeled by following the principles of the ENApp DOPF algorithm. ENApp outperforms the other DOPF algorithms in terms of convergence speed and requires fewer macro iterations [12]. A taxonomy table to compare the existing studies and the present work is provided in Table I. The specific contributions of this paper are listed below:

1) A MPOPF framework is proposed for distribution systems consisting of DERs and batteries. The integer variables related to battery charging/discharging are avoided by adding a "Battery Loss" cost term in the objective function. The loss term will ensure the non-occurrence of simultaneous charging/discharging operations.
2) The original MPOPF framework is solved in a distributed manner by following the principles of the ENApp-based distributed OPF. This provides faster convergence and requires less solution time compared to the traditional MPCOPF.
3) Detailed comparative analyses between traditional MPCOPF and the proposed MPDOPF are done using the IEEE 123 bus test system and the benefits of the proposed approach are demonstrated. ACOPF feasibility validation is also performed by implementing the derived controls into an OpenDSS model of the test system.

II. PROBLEM FORMULATION

A. Notations

In this study, the distribution system is modeled as a tree (connected graph) with N number of buses (indexed with i, j, and k); the study is conducted for T time steps (indexed by t), each of interval length Δt. The sets of buses with DERs and batteries are D and B respectively, such that $D, B \subseteq N$. A directed edge from bus i to j in the tree is represented by ij and the set for edges is given by $\mathcal{L}$. Line resistance and reactance are r_{ij} and x_{ij}, respectively. Magnitude of the current flowing through the line at time t is denoted by I_{ij}^t and $l_{ij}^t = \left(I_{ij}^t\right)^2$. The voltage magnitude of bus j at time t is given by V_j^t and $v_j^t = \left(V_j^t\right)^2$. Apparent power demand at a node j at time t is $s_{L_j}^t$ $(= p_{L_j}^t + jq_{L_j}^t)$. The active power generation from the DER present at bus j at time t is denoted by $p_{D_j}^t$ and controlled reactive power dispatch from the DER inverter is $q_{D_j}^t$. DER inverter capacity is $S_{D_{R_j}}$. The apparent power flow through line ij at time t is S_{ij}^t $(= P_{ij}^t + jQ_{ij}^t)$. The real power flowing from the substation into the network is denoted by P_{Subs}^t and the associated cost involved per kWh is C^t. The battery energy level is B_j^t. Charging and discharging active power from battery inverter (of apparent power capacity $S_{B_{R_j}}$) are denoted by $P_{c_j}^t$ and $P_{d_j}^t$, respectively and their associated efficiencies are η_c and η_d, respectively. The energy capacity of the batteries is denoted by B_{R_j}, and the rated battery power is $P_{B_{R_j}}$. soc_{min} and soc_{max} are fractional values for denoting safe soc limits of a battery about its rated state-of-charge (soc) capacity. The reactive power support of the battery inverter is indicated by $q_{B_j}^t$.

B. MPCOPF with Batteries

The OPF problem aims to minimize two objectives as shown in (1). The first term in (1) aims to minimize the total energy cost for the entire horizon. Including the 'Battery Loss' cost as the second term ($\alpha > 0$) helps eliminate the need for binary (integer) variables typically used to prevent simultaneous charging and discharging. The resulting OPF problem is a non-convex optimization problem [19].

$$\min \sum_{t=1}^{T} \Bigg[C^t P_{Subs}^t \Delta t + \alpha \sum_{j \in \mathcal{B}} \Big\{ (1-\eta_C) P_{C_j}^t + \left(\frac{1}{\eta_D} - 1 \right) P_{D_j}^t \Big\} \Bigg] \tag{1}$$

Subject to the constraints (2) to (12) as given below:

$$\sum_{(j,k) \in \mathcal{L}} \left\{ P_{jk}^t \right\} - \left(P_{ij}^t - r_{ij} l_{ij}^t \right) = \left(P_{d_j}^t - P_{c_j}^t \right) + p_{D_j}^t - p_{L_j}^t \tag{2}$$

$$\sum_{(j,k)\in\mathcal{L}} \{Q_{jk}^t\} - (Q_{ij}^t - x_{ij} l_{ij}^t) = q_{D_j}^t + q_{B_j}^t - q_{L_j}^t \quad (3)$$

$$v_j^t = v_i^t - 2(r_{ij}P_{ij}^t + x_{ij}Q_{ij}^t) + \{r_{ij}^2 + x_{ij}^2\} l_{ij}^t \quad (4)$$

$$(P_{ij}^t)^2 + (Q_{ij}^t)^2 = l_{ij}^t v_i^t \quad (5)$$

$$P_{Subs}^t \geq 0 \quad (6)$$

$$v_j^t \in [V_{min}^2, V_{max}^2] \quad (7)$$

$$q_{D_j}^t \in \left[-\sqrt{{S_{D_{R,j}}}^2 - {p_{D_j}^t}^2}, \sqrt{{S_{D_{R,j}}}^2 - {p_{D_j}^t}^2}\right] \quad (8)$$

$$B_j^t = B_j^{t-1} + \Delta t \eta_c P_{c_j}^t - \Delta t \frac{1}{\eta_d} P_{d_j}^t \quad (9)$$

$$P_{c_j}^t, P_{d_j}^t \in \left[0, P_{B_{R_j}}\right], \quad B_j^0 = B_j^T \quad (10)$$

$$q_{B_j}^t \in \left[-\sqrt{0.44} P_{B_{R,j}}, \sqrt{0.44} P_{B_{R,j}}\right] \quad (11)$$

$$B_j^t \in [soc_{min} B_{R,j}, soc_{max} B_{R,j}] \quad (12)$$

A branch power flow model, given by (2) to (5), is used to represent power flow in distribution system. Constraints (2) and (3) model the active and reactive power balance at node j, respectively. The KVL equation for branch (ij) is represented by (4), while the equation describing the relationship between current magnitude, voltage magnitude and apparent power magnitude for branch (ij) is given by (5). Backflow of real power into the substation from the distribution system is avoided using the constraint (6). The allowable limits for bus voltages are modeled via (7). (8) describes the reactive power limits of DER inverters. The trajectory of the battery energy versus time is given by (9) (this is a time-coupled constraint). Battery charging and discharging powers are limited by the battery's rated power capacity, as given by (10). (10) also says that the initial and final energy levels for battery must be the same at the end of the optimization time horizon. Every battery's reactive power is also constrained by the corresponding inverter's rated capacity, modeled in (11). For the safe and sustainable operation of the batteries, the energy B_j^t is constrained to be within some percentage limits of the rated battery SOC capacity, modeled using (12)

C. ENApp based MPDOPF with Batteries

Assuming the presence of a feasible solution for the MP-COPF problem, the MPDOPF is formulated by decomposing the distribution system into multiple small areas. In this paper, the interaction between the two areas will follow the principle of ENApp algorithm. The ENApp algorithm leverages the radial topology of the distribution network to solve the network-level optimization problem in a distributed manner. Each area has a local controller (LC) that solves its specific local optimization problem. The local optimization problem will be the same MPOPF as described in Section II-B but defined using only the variables and parameters specific for the corresponding area. The boundary buses between two areas are accounted as voltage sources for downstream areas and load buses for upstream areas. By knowing the upstream voltage and downstream load data, the LCs will solve their area-specific MPOPF in parallel. Once LC problem converges, the downstream and upstream LCs inform power flows and voltage data to their respective upstream and downstream areas. The LCs will again solve their local MPOPF and exchange the updated boundary variables with their neighbors. This iterative process terminates after a convergence is achieved at all boundary buses. Comprehensive details of the ENApp algorithm are available in [12]. Note that for the case of multi-period optimization with T time steps, each area exchanges a data vector containing $2T$ boundary variables with its neighboring areas. This includes voltage and power flow data for each of the T time steps.

TABLE II: Parameter values

Parameter	Value
V_{min}, V_{max}	0.95, 1.05
$p_{D_{R_j}}$	$0.33 p_{L_{R_j}}$
$S_{D_{R_j}}$	$1.2 p_{D_{R_j}}$
$P_{B_{R_j}}$	$0.33 p_{L_{R_j}}$
$S_{B_{R_j}}$	$1.2 P_{B_{R_j}}$
B_{R_j}	$T_{fullCharge} \times P_{B_{R_j}}$
$T_{fullCharge}$	4 h
Δt	1 h
η_c, η_d	0.95, 0.95
soc_{min}, soc_{max}	0.30, 0.95
α	0.001

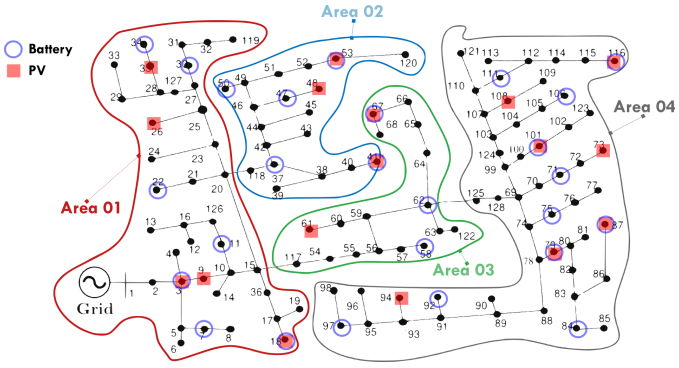

Fig. 1: IEEE 123 node system divided into four areas

III. Case Study Demonstration

A. Simulation Data: IEEE 123 Bus Test System

The case studies are conducted on the balanced three-phase version of the IEEE 123 bus test system, which has 85 Load Nodes. Additionally, 20% (17) and 30% (26) of these load nodes also contain reactive power controllable PVs and BESS, respectively. Their ratings are as per Table II. To demonstrate the effectiveness of the proposed algorithm, the test system is divided into four areas as shown in Figure 1. It is assumed that a horizon-wide forecast for loads p_L^t, solar power output p_D^t and cost of substation power C^t is available to the distribution system operator. Initially, the study is carried out for 5 hours with input data shown in Figure 2. The five-hour workflow is described below.

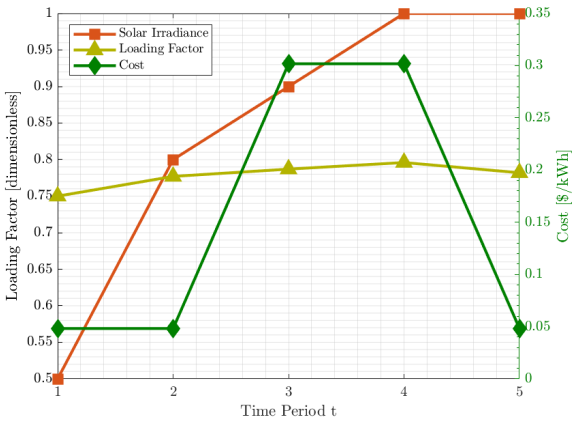

Fig. 2: Forecasts for demand power, irradiance and cost of substation power over a 5 hour horizon

B. Simulation Workflow

All simulations were set up in MATLAB 2023a including both the high level algorithms as well as calls to the optimization solver. MATLAB's `fmincon` function was used to parse the nonlinear nonconvex optimization problem described by (1) to (12) in tandem with the SQP optimization algorithm to solve it. From the completed simulations, the resultant optimal control variables were obtained, and were passed through an OpenDSS engine (already configured with system data and forecast values) in order to check for the ACOPF feasibility of the results. The associated code may be found in [20]. As the IEEE 123 bus system is decomposed into 4 areas, so the total number of variables exchanged at each iteration for the 5-hour simulation of the MPDOPF is $2 * 3 * 5 = 30$.

In the following subsections, the proposed MPDOPF algorithm is compared against the MPCOPF algorithm in terms of resultant optimal control variables, optimality gap in the objective function, and computational performance. Secondly, the resultant control variables are tested for ACOPF feasibility against OpenDSS. Section III-C describes the comparison over a 5 hour horizon with an additional focus on describing the workflow of the MPDOPF algorithm. Section III-D describes the comparison over a 10 hour horizon to test for the scalability of the MPDOPF algorithm.

C. Simulation Results

Table III depicts a comparison between MPCOPF and MPDOPF in their problem scope, results and computational performance.

1) Largest Subproblem vs. Computational Performance: This first section of the Table III, 'largest subproblem' provides specifics of the 'computational bottleneck' encountered by either algorithm during its course. As described in Section II-C, the bottleneck represents the OPF subproblem which is computationally the most intensive and thus is a key indicator of the expected time the algorithm will take to complete. As can be seen in the third section 'Computation', there is more than a 10x speedup in computation time with MPDOPF,

TABLE III: Comparative analyses between MPCOPF and MPDOPF - 5 time-period horizon

Metric	MPCOPF	MPDOPF
Largest subproblem		
Decision variables	3150	1320
Linear constraints	5831	2451
Nonlinear constraints	635	265
Simulation results		
Substation power cost ($)	576.31	576.30
Substation real power (kW)	4308.28	4308.14
Line loss (kW)	75.99	76.12
Substation reactive power (kVAR)	574.18	656.24
PV reactive power (kVAR)	116.92	160.64
Battery reactive power (kVAR)	202.73	76.01
Computation		
Number of Iterations	-	5
Total Simulation Time (s)	521.25	49.87

even though 5 such iterations were performed, totalling to 20 OPF calls over the 4 areas of the test system.

2) Optimality of Objective Function and Control Variables: The second section of the Table III i.e. 'Simulation results' showcases that MPDOPF provides almost zero optimality gap (same values for Substation Power Cost, the objective function). Interestingly, there is a significant difference in the suggested optimal reactive power control values for inverters associated with DERs and batteries (results aggregated over all components over the horizon for conciseness). This highlights the fact that a nonconvex nonlinear optimization problem may not necessarily have a unique global optimal point. There is a possibility of having multiple feasible solutions with the same objective function value.

3) ACOPF Feasibility Analysis: Table IV showcases the ACOPF feasibility of the control values suggested by the MPDOPF algorithm. The first section 'Full horizon' describes the respective output variables for the entire horizon from MPDOPF and OpenDSS. The second section 'Max. all-time discrepancy' stores the highest discrepancy between key state/output variables for all components across any time between MPDOPF and OpenDSS. In both sections, the discrepancies are small enough to warrant the feasibility of the obtained solution.

TABLE IV: ACOPF feasibility analyses - 5 hour

Metric	MPDOPF	OpenDSS
Full horizon		
Substation real power (kW)	4308.14	4308.35
Line loss (kW)	76.12	76.09
Substation reactive power (kVAR)	656.24	652.49
Max. all-time discrepancy		
Voltage (pu)	0.0002	
Line loss (kW)	0.0139	
Substation power (kW)	0.3431	

To ensure that battery charging and discharging complementarity is respected without relying on integer constraints, the battery charging and discharging profiles were carefully examined. The results confirm this complementarity, as illustrated in Figure 3 as one such example.

4) Workflow Analysis: The workflow of the MPDOPF algorithm, which involves the exchange of boundary variables

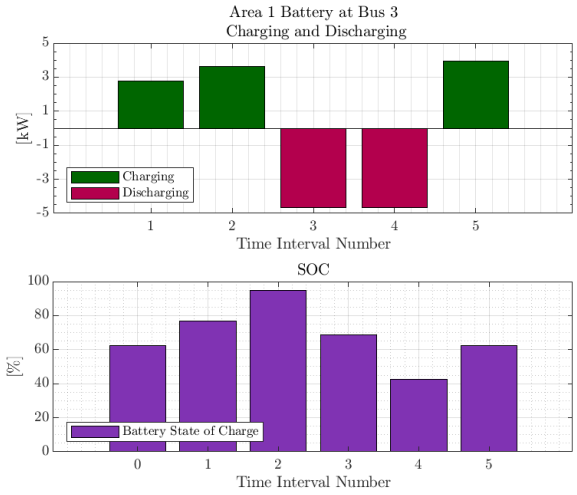

Fig. 3: Charging-discharging and SOC graphs for battery at bus 3 located in Area 1 obtained by MPDOPF

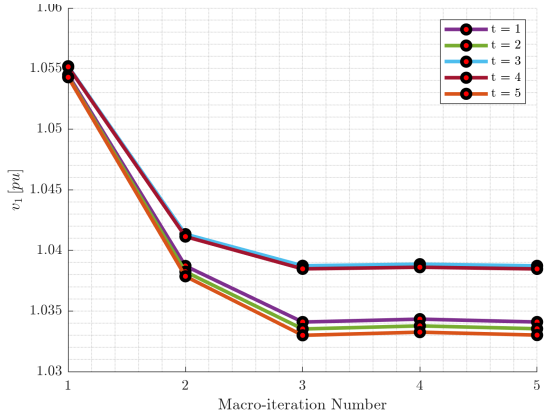

Fig. 4: Shared voltage data from Area 1 to Area 2.

between parent-child area pairs, can be seen in the convergence plots in Figures 4 and 5, with each line graph representing a particular time period in both plots. Similarly, the convergence of the objective function to its optimal value with every iteration is shown by Figure 6. It is noted that, though at the starting the values are not at their optimal values, but with rolling iterations the values move to their optimum conditions and converge after 5 macro iterations.

D. Scalability Analysis

To demonstrate the effectiveness of the proposed algorithm over a bigger horizon to demonstrate scalability, further simulations were run for a 10 hour horizon. Figure 7 shows the forecasted profiles for load, solar irradiance and cost of substation power over the 10-hour horizon. The simulation results are summarized in Table V and Table VI.

From the comparison against MPCOPF in Table V, it can again be seen that MPDOPF is able to converge to the same optimal solution as MPCOPF. The computational speed up is even more pronounced than for the 5 time-period simulation. It is noted that the solution time increased drastically for MPCOPF with the increasing length of the study horizon.

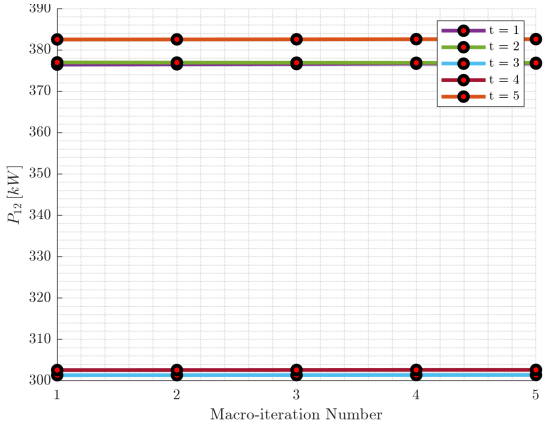

Fig. 5: Shared real power data from Area 4 into Area 2.

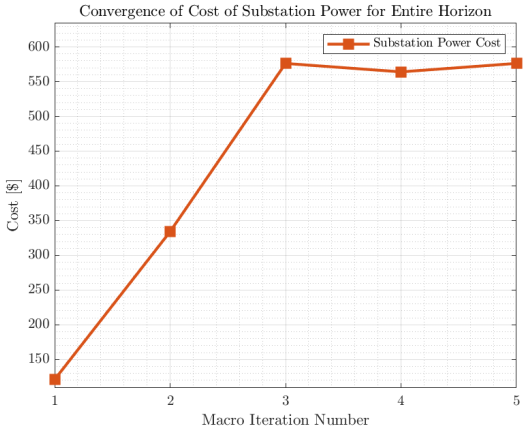

Fig. 6: Convergence of objective function value with each MPDOPF iteration

However, the solution time increment for MPDOPF is comparatively less. Therefore, the proposed spatially distributed MPOPF framework is scalable to some extent.

TABLE V: Comparison between MPCOPF and MPDOPF - 10 hour

Metric	**MPCOPF**	**MPDOPF**
Largest subproblem		
Decision variables	6300	2640
Linear constraints	11636	4891
Nonlinear constraints	1270	530
Simulation results		
Substation power cost ($)	1197.87	1197.87
Substation real power (kW)	8544.28	8544.04
Line loss (kW)	148.67	148.94
Substation reactive power (kVAR)	1092.39	1252.03
PV reactive power (kVAR)	222.59	139.81
Battery reactive power (kVAR)	388.52	310.94
Computation		
Number of Iterations	-	5
Total Simulation Time (s)	4620.73	358.69

Again, as can be seen in Table VI comparison against OpenDSS has yielded small discrepancies, attesting to the feasibility of the solution.

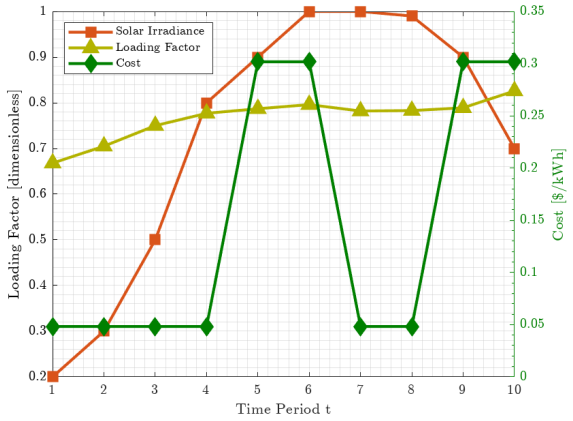

Fig. 7: Forecasts for demand power, irradiance and cost of substation power over a 10 hour Horizon

TABLE VI: ACOPF feasibility analyses - 10 hour

Metric	MPDOPF	OpenDSS
Full horizon		
Substation real power (kW)	8544.04	8544.40
Line loss (kW)	148.94	148.87
Substation reactive power (kVAR)	1252.03	1243.36
Max. all-time discrepancy		
Voltage (pu)	0.0002	
Line loss (kW)	0.0132	
Substation power (kW)	0.4002	

IV. Conclusions

This study aims to develop a computationally-efficient approach to solve multi-period optimal power flow problems (MPOPF) in distribution systems to coordinate DERs and BESS. Specifically, the authors propose a spatially distributed approach utilizing the ENApp algorithm to solve the MPOPF problem. The effectiveness of the proposed distributed algorithm is validated via simulations on the IEEE 123 bus test system. Simulation results demonstrate that the proposed distributed approach achieves solutions that are AC-feasible and nearly optimal (approaching the solutions obtained from equivalent centralized formulations), while significantly reducing computational costs. This highlights the efficacy of spatial decomposition in reducing solution times for MPOPF problems. However, it is important to note that even the proposed spatially distributed MPOPF algorithm encounters computational complexities when optimizing over longer time horizons. In the future, the authors plan to investigate integrating spatial and temporal decomposition techniques to address scalability issues in time-coupled multi-period OPF problems.

V. Acknowledgement

The authors acknowledge the financial support provided by the Department of Energy (DOE) for the project named 'Spokane Connected Communities' under contract number DE-EE0009775.

References

[1] T. Gangwar, N. P. Padhy, and P. Jena, "Storage allocation in active distribution networks considering life cycle and uncertainty," IEEE Trans. Ind. Inform., vol. 19, no. 1, pp. 339–350, Jan. 2023.

[2] S. Paul and N. P. Padhy, "Real-time advanced energy-efficient management of an active radial distribution network," IEEE Syst. J., vol. 16, no. 3, pp. 3602–3612, Sept. 2022.

[3] W. Wei, J. Wang, and L. Wu, "Distribution optimal power flow with real-time price elasticity," IEEE Trans. Power Syst., vol. 33, no. 1, pp. 1097–1098, Jan. 2018.

[4] M. M.-U.-T. Chowdhury, B. D. Biswas, and S. Kamalasadan, "Second-order cone programming (socp) model for three phase optimal power flow (opf) in active distribution networks," IEEE Trans. Smart Grid, vol. 14, no. 5, pp. 3732–3743, 2023.

[5] Z. Guo, W. Wei, L. Chen, Z. Dong, and S. Mei, "Parametric distribution optimal power flow with variable renewable generation," IEEE Trans. Power Syst., vol. 37, no. 3, pp. 1831–1841, May 2022.

[6] H. Yuan, F. Li, Y. Wei, and J. Zhu, "Novel linearized power flow and linearized opf models for active distribution networks with application in distribution lmp," IEEE Trans. Smart Grid, vol. 9, no. 1, pp. 438–448, Jan. 2018.

[7] A. R. Di Fazio, C. Risi, M. Russo, and M. De Santis, "Decentralized voltage optimization based on the auxiliary problem principle in distribution networks with ders," Appl. Sci., vol. 11, no. 4509, pp. 1–24, 2021.

[8] W. Zheng, W. Wu, B. Zhang, H. Sun, and Y. Liu, "A fully distributed reactive power optimization and control method for active distribution networks," IEEE Trans. Smart Grid, vol. 7, no. 2, pp. 1021–1033, Mar. 2016.

[9] P. Wang, Q. Wu, S. Huang, C. Li, and B. Zhou, "Admm-based distributed active and reactive power control for regional ac power grid with wind farms," J. Modern Power Syst. Clean Energy, vol. 10, no. 3, pp. 588–596, May 2022.

[10] B. D. Biswas, M. S. Hasan, and S. Kamalasadan, "Decentralized distributed convex optimal power flow model for power distribution system based on alternating direction method of multipliers," IEEE Trans. Ind. Appl., vol. 59, no. 1, pp. 627–640, Jan.-Feb. 2023.

[11] S. Paul, B. Ganguly, and S. Chatterjee, "Nesterov-type accelerated admm (n-admm) with adaptive penalty for three-phase distributed opf under non-ideal data transfer scenarios," in 2023 IEEE 3rd International Conference on Smart Technologies for Power, Energy and Control (STPEC), 2023, pp. 1–6.

[12] R. Sadnan and A. Dubey, "Distributed optimization using reduced network equivalents for radial power distribution systems," IEEE Trans. Power Syst., vol. 36, no. 4, pp. 3645–3656, Jul. 2021.

[13] A. Gabash and P. Li, "Active-reactive optimal power flow in distribution networks with embedded generation and battery storage," IEEE Trans. Power Syst., vol. 27, no. 4, pp. 2026–2035, Nov. 2012.

[14] M. I. Alizadeh and F. Capitanescu, "A tractable linearization-based approximated solution methodology to stochastic multi-period ac security-constrained optimal power flow," IEEE Trans. Power Syst., vol. 38, no. 6, pp. 5896–5908, 2023.

[15] M. Usman and F. Capitanescu, "Three solution approaches to stochastic multi-period ac optimal power flow in active distribution systems," IEEE Trans. Sustain. Energy, vol. 14, no. 1, pp. 178–192, 2023.

[16] F. H. Aghdam, M. W. Mudiyanselage, B. Mohammadi-Ivatloo, and M. Marzband, "Optimal scheduling of multi-energy type virtual energy storage system in reconfigurable distribution networks for congestion management," Applied Energy, vol. 33, no. 120569, pp. 1–17, 2023.

[17] J. Zhang and Y. He, "Fast solving method for two-stage multi-period robust optimization of active and reactive power coordination in active distribution networks," IEEE Access, vol. 11, pp. 30 208–30 222, 2023.

[18] C. Wu, W. Gu, S. Zhou, and X. Chen, "Coordinated optimal power flow for integrated active distribution network and virtual power plants using decentralized algorithm," IEEE Trans. Power Syst., vol. 36, no. 4, pp. 3541–3551, Jul. 2021.

[19] N. Nazir and M. Almassalkhi, "Guaranteeing a Physically Realizable Battery Dispatch Without Charge-Discharge Complementarity Constraints," IEEE Trans. Smart Grid, vol. 14, no. 3, pp. 2473–2476, Sep. 2021.

[20] "MultiPeriod-DistOPF-Benchmark," Jul. 2024, [Online; accessed 15. Jul. 2024]. [Online]. Available: https://github.com/Realife-Brahmin/MultiPeriod-DistOPF-Benchmark